

Metastable polymeric nitrogen nanotube from a zigzag sheet phase and first-principles calculations

Anguang Hu,¹ Fan Zhang,¹ and Tom Woo²

¹Defence R&D Canada-Suffield, P.O. Box 4000, Medicine Hat, Alberta, Canada T1A 8K6

²Department of Chemistry, University of Ottawa, D'Iorio Hall, Ottawa, Ontario, Canada K1N 6N5

(Received 14 September 2009; revised manuscript received 3 August 2010; published 7 September 2010)

A metastable zigzag sheet phase of polymeric nitrogen has been theoretically predicted in phase transformations from the theoretically predicted structures of a denser nitrogen molecular zeta phase. Built from this sheet structure, a polymeric nitrogen nanotube is postulated to comprise 18 zigzag single-bonded N_6 motifs and computationally modeled using first-principles density-functional theory. The metastability of the nitrogen tube was demonstrated with structural optimization calculations, phonon dispersion calculations, and finite-temperature first-principles molecular-dynamics simulations. Band-structure calculations show that this metastable polymeric nitrogen nanotube is an insulator with a band gap of about 3.0 eV.

DOI: [10.1103/PhysRevB.82.125410](https://doi.org/10.1103/PhysRevB.82.125410)

PACS number(s): 61.50.Ah, 61.46.Fg, 61.66.Bi, 71.15.Mb

I. INTRODUCTION

At near-ambient conditions, nitrogen as the major constituent of air exists exclusively in a molecular form (i.e., as a gas, liquid, or molecular solid) due to the very strong triple bond of N_2 molecules, the second strongest only to the CO bond. The energy difference between the single- or double-bonded nitrogen and the triple-bonded nitrogen systems suggests that a huge amount of energy can be stored in single-bonded polymeric nitrogen provided it is metastable. Thus, polymeric nitrogen was considered as one of potential high-energy density materials. In 1992, Mailhot *et al.* theoretically predicted cubic gauche (CG) nitrogen to be the most probable form of high-pressure polymeric nitrogen.¹ Its existence was proved by Eremets *et al.* in 2004 using diamond cell anvil experiments at 110 GPa and 2000 K.² This new member of single-bonded nitrogen materials has unique properties including an energy density of about 27.89 kJ/g and remains metastable at lower pressures down to a limit of 42 GPa. Since then a number of new metastable polynitrogen phases have been computationally predicted^{3,4} while numerous finite clusters of nitrogen were considered and computationally modeled using *ab initio* methods during the last decade.⁵ Stable dodecahedral N_{20} was also predicted at various levels of theories.^{6–8} A stable nanoscale fullerene-like N_{60} structure was found using a semiempirical computational method but has not yet been confirmed by a subsequent *ab initio* calculation.^{9,10}

Theoretically, polymeric nitrogen may have a number of solid-state covalent phases. Depending on the repulsion of electron lone pairs, the energetically favorable polymeric nitrogen phases in general are characterized by the electron lone pairs separated as much as possible, thus leading to a great reduction in repulsion of lone pairs from the single-bonded N-N moiety.^{1,11} In polymeric nitrogen CG, for instance, the lp-N-N-lp dihedral angle is about 107° (lp represents the lone pair), which results in gauche angle effects for electron lone pairs.^{1,11} Black phosphorus (BP), arsenic (A7), and layered boat-shape (LB) polymeric nitrogen phases all exhibit layered structures; their internal energies can be related not only to the gauche N-N bond but also to *trans* and

cis N-N bonds in order to adapt two-dimensional characters. These layered polymeric nitrogen structures, however, are unstable at lower pressures because the bonds between chains are the weakest in the structure. These weakest bonds break at the ambient pressure, leading to the separation of chains.¹²

Since the discovery of carbon nanotubes in 1991,¹³ the fact that a graphitic sheet is the basic building block of all carbon nanotubes has promoted synthesis studies of a class of new nanotubes derived from stable layered structures of various materials. Numerous examples of nanotubes have been constructed from either main group elements or transition metals. For instance, single-walled stoichiometric boron-nitrogen nanotubes, isoelectronic with carbon nanotubes, were synthesized¹⁴ and have been a subject of *ab initio* electronic-structure calculations.¹⁵ The graphitelike planar structures of boron nitride can be formed as a basic block to build boron nitride nanotubes. Pure boron sheets and the derived nanotubes have been predicted where the boron sheets are not planar and the nanotube walls are “kinked.”¹⁶ Nonstoichiometric $B_xC_yN_z$ (Refs. 17 and 18) and CN_x (Ref. 19) nanotubes have also been studied and synthesized. Phosphorous nanotubes based on the two-dimensional black phosphorus allotrope^{20,21} and phosphorus fullerenes²² have been reported. The question naturally arises is whether the synthesis of nitrogen nanotubes and fullerenes is possible. Nitrogen fullerenes⁹ were previously suggested together with finite-size nitrogen nanoneedles and nanotubes²³ but to the authors’ knowledge, studies of pure polymeric nitrogen nanotubes have not reported in the literature.

In this paper, first-principles calculation results are presented to reveal a stable layered polymeric nitrogen phase—a zigzag sheet at lower pressures, and a pure polymeric nitrogen nanotube constructed with 18 zigzag N_6 motifs along with the structural properties, metastability and electronic structures of this nanotube.

II. TECHNICAL DETAILS

The present work is based on the calculations of density-functional theory with the Perdew-Burke-Ernzerhof

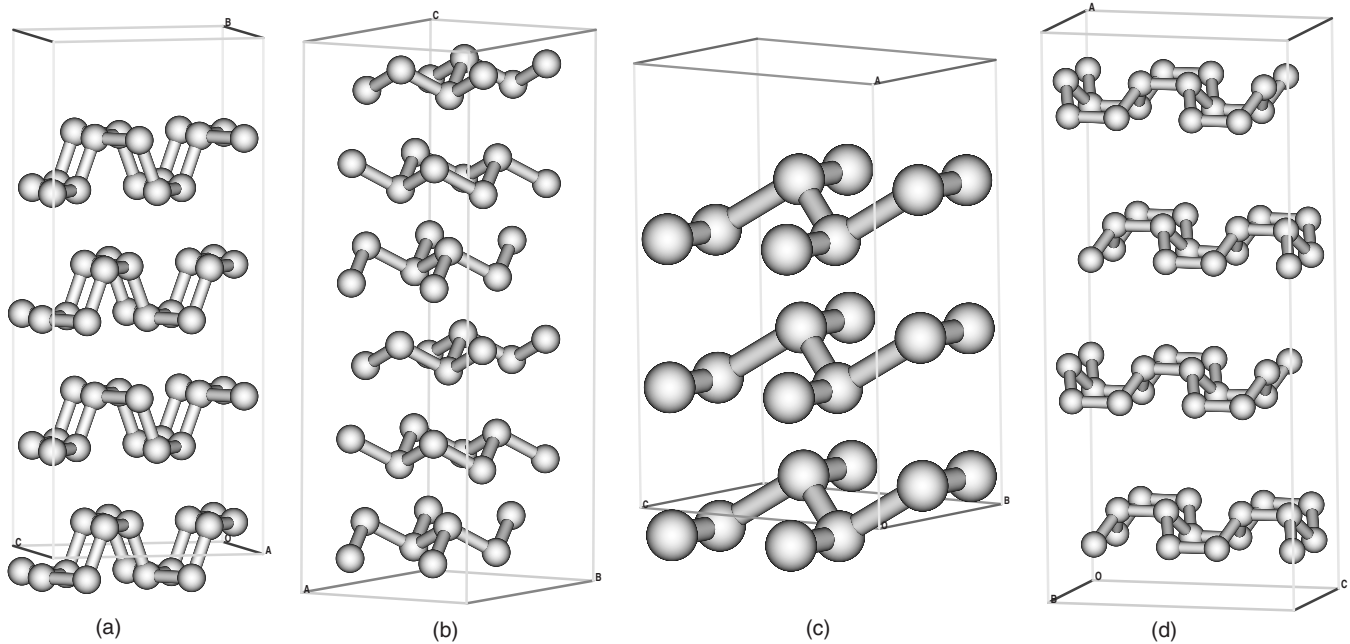


FIG. 1. Crystal structures of layered polymeric nitrogen; (a) BP with space group 63: a view with a $2 \times 2 \times 2$ supercell, (b) A7 with space group 167: a view with a $2 \times 2 \times 2$ supercell and (c) LB with space group 11: a view with a $3 \times 1 \times 2$ supercell and (d) ZS with space group 62: a view with a $2 \times 2 \times 2$ supercell.

exchange-correlation functional²⁴ implemented in the SIESTA (Ref. 25) and VASP (Ref. 26) programs. The norm-conserving pseudopotentials²⁷ in the parameterization of Troullier-Martins²⁸ were used in the reference configuration of nitrogen [He] $2s^2 2p^3$ with a cutoff radius of 1.24 Å. A customized SIESTA basis set of numerical “double zeta with polarization” SEISTA basis set²⁹ was used. A 20 Å cutoff for k -point sampling was employed based on the convergence of geometries and relative thermodynamic stabilities. The real-space mesh cutoff was set to 200.0 Ry using the SIESTA program. VASP was used with the projector-augmented wave method of Blöchl to treat the core states.³⁰ A plane-wave cutoff of 80 Ry was used and the Brillouin-zone integration was performed using a Monkhorst-Pack grid with the same number of k -point sampling generated by a 20 Å cutoff using SIESTA. In both SIESTA and VASP programs, a variable-cell-shape conjugate gradient method under constant pressure was applied to the minimization of the geometries, and the standard Verlet integrator with Nose-Parrinello-Raman method was used for the molecular dynamics with a 1 fs time step.

For the stability of this pure polymeric nitrogen nanotube, we calculated the phonon-dispersion relation following the scheme proposed by Kunc and Martin.³¹ Within this method, a $1 \times 1 \times 3$ supercell is first created and all irreducible directions within the cell are searched for. This supercell contains 324 nitrogen atoms with sufficient size to limit the forces inside the cell. After this, each plane of atoms perpendicular to each direction is displaced along the three degrees of freedom to calculate the forces exerted on all atoms by the displacement. The force constant matrix is then constructed and used to calculate the dynamical matrix for the primitive cell for different \mathbf{k} vectors along the high-symmetry axes. The

square roots of the eigenvalues for the dynamical matrix give the frequencies of the phonon modes for each \mathbf{k} . The imaginary frequencies correspond to directions of barrierless phase transitions indicating instability of the phase.

III. RESULTS AND DISCUSSION

Figures 1(a)–1(d) show theoretically predicted layered structures of polymeric nitrogen. These structures include BP, A7, LB, and a new layered polymeric nitrogen phase, which we name ZS since it is featured with a perfect zigzag sheetlike structure. This phase was transformed from either $Pbcn$ or $P2_12_12_1$ molecular nitrogen zeta phases³² at about 190 GPa with simple instantaneous homogenous isotropic compression simulations. This predicted transition pressure is consistent with the overpressure of ~ 200 GPa required to cause a transition in some experiments with cold compression.³³ The primitive cell of ZS is triclinic with $Pnma$ space group. At the ambient pressure, the primitive cell vector lengths are $a=8.6637$ Å, $b=2.3340$ Å, $c=3.8588$ Å and angles are $\alpha=\beta=\gamma=90.0^\circ$, respectively. The equivalent atomic positions, $4c(x, 0.2500, z)$ Wyckoff positions, could be recovered from (0.8014, 0.7500, 0.0550) and (0.6985, 0.7500, 0.1672) in fractional coordinates by the use of symmetry. Its pressure boundary range is from the ambient pressure to 320 GPa in structural optimization calculations. The space between two neighboring layers at the ambient pressure is about 3.656 Å, along the $[0,1,0]$ -direction projection, it shows perfect zigzag chains characterized with a 1.531 Å bond length and a 99.29° bond angle. In contrast to the unstable BP, A7, and LB layered structures in which the weakest bond between chains breaks at low pressures,¹² the ZS phase is stable even at the ambient pres-

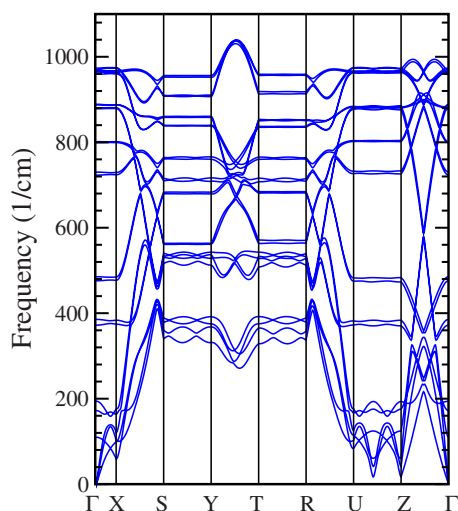


FIG. 2. (Color online) Phonon dispersion of ZS calculated at ambient pressure using a $3 \times 3 \times 3$ supercell and a $2 \times 6 \times 2$ k -point mesh.

sure because the connection bond between zigzag chains has a length of 1.496 Å and is therefore not the weakest bond of the structure. The calculated phonon dispersion at the ambient pressure is shown in Fig. 2. There are no negative frequency modes, thus indicating its stability at the ambient pressure. Moreover, first-principles molecular-dynamics simulations also show its metastability at the room temperature.

Pure polymeric nitrogen nanotubes were then constructed based on the ZS layered polymeric nitrogen phase. Figure 3(a) shows a simulated unit cell of the constructed polymeric nitrogen nanotube with lattice constants, $a=6.9011$ Å, $b=30.2296$ Å, and $c=29.4123$ Å, and lattice angles, $\alpha=\beta=\gamma=90.0^\circ$. The lattice constants and angles were all optimized together with atomic positions using the variable-cell-shape conjugate gradient method. At the end of optimization, the simulated cell showed symmetry with space group $Pmma$ though no any symmetry constraints were applied in the simulations. In terms of structural properties, it was found that this nitrogen nanotube consists of 18 zigzag N_6 which are connected by nitrogen single bonds, shown in Figs. 3(b) and 3(c). There are two types of N_6 zigzag motifs; the first one is characterized with a bond length of 1.509 Å and an angle of 99.28° while a bond of 1.444 Å and an angle of 105.57° are found for the second one. Chains 1 and 10 in Fig. 3(b) belong to the second motif and the rest are the first one. The chain-connection bond lengths vary depending on the curvature of the tube surface, following the order of 1.544 Å, 1.522 Å, 1.518 Å, 1.522 Å and 1.544 Å from chain 1 to chain 6, respectively. Obviously, the bond lengths of zigzag chains are all larger than the chain-connection bond lengths. In comparison with polymeric sheet structures of BP, A7, and LB, this nanotube would appear to be composed of four stripes from the sheets of A7 linked by short stripes of BP and LB based on polymorphism of the tube surface. However, this is not true since the connection bonds between the chains are no longer the weakest bonds in the structure as found in the PB, A7, and LB phase. In fact, the

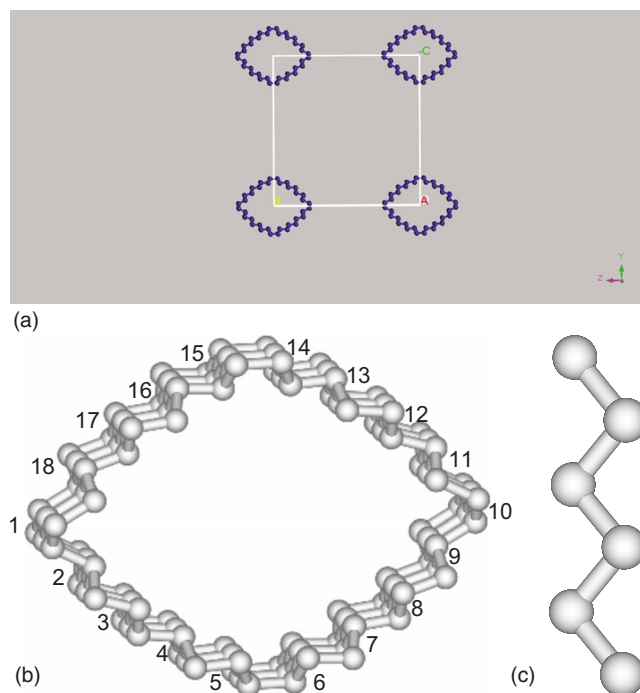


FIG. 3. (Color online) The polymeric nitrogen nanotube; (a) simulated unit cell of nitrogen tube with space group 51: a view along [100], (b) the cross section of the nitrogen nanotube showing 18 zigzag N_6 motifs, and (c) a zigzag N_6 motif.

stability of this nitrogen nanotube is related to its structural properties, characterized by zigzag motifs and nonweakest bonds between chains. It has already been observed from previous simulations that zigzag chainlike polymeric nitrogen phases were always energetically more stable than other chainlike ones such as *trans-cis* chainlike phases.^{4,12}

In order to examine the metastability of this nanotube, we performed a full phonon-dispersion curve calculation shown in Figs. 4(a)–4(d). A lack of negative modes in 324 phonon-dispersion bands establishes the structural metastability of the tube at the ambient pressure. Moreover, the lowest frequency of acoustic branches is about 120 cm^{-1} , which is horizontal at the zone boundary position X, indicating no weaker lattice modes. While the phonon-dispersion calculation rigorously confirmed the metastability of the nitrogen tube, it does not elaborate the lifetime of this metastable state. To further probe the metastability, first-principles molecular dynamics runs were performed at the room temperature using SIESTA due to its much higher efficiency. Several independent runs were initiated at starting configurations with randomly displaced coordinates by 5% of their interatomic distance around the optimal positions and velocities randomly chosen from the Maxwell distribution. The cumulative time of all the runs was 10 ps. All these calculations showed the stability of this nitrogen nanotube at the ambient condition. Based on the structural properties shown above, one can see that like the other purely single-bonded polymeric nitrogen phases, the stability of the tube is governed to a large extent by the repulsion of lone pairs. The electronic density and electron localization calculations showed that the neighboring nitrogen lone pairs are generally pointing away

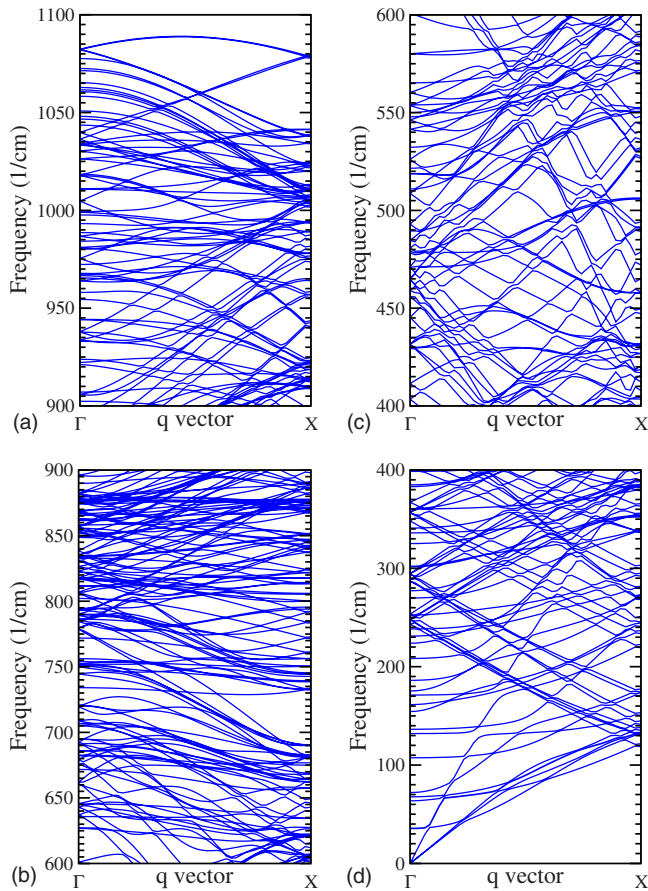


FIG. 4. (Color online) Phonon dispersion of the nitrogen nanotube calculated at ambient pressure. There are 324 phonon dispersion bands. The dispersion relations are; frequencies (a) above 900 cm^{-1} , (b) between 900 and 600 cm^{-1} , (c) between 600 and 400 cm^{-1} , and (d) between 400 and 0 cm^{-1} .

from each other. The exceptions to this are the segments between chain 5 and 6 or between chain 14 and 15 by symmetry, which leads to the longest bond lengths between the zigzag chains in the tube. In our calculations, some nitrogen nanotubes with smaller diameters were also found by structure optimization simulations. However, further calculations on the metastability show that they were dynamic unstable due to negative frequency modes. In general, there were more the weakest bonds between chains for nitrogen nanotubes with smaller diameters. Finally, we calculated the nanotube band structure shown in Fig. 5. Like the other single-bonded polymeric nitrogen phases again, the tube is an insulator with an about 3.0 eV band gap. The enthalpy of this nitrogen tube calculated at the ambient pressure is about 0.1 eV/atoms lower than the value of ZS phase but 0.2 eV/atoms higher than the value of CG phase, indicating that this tube is energetically favorable over ZS at the ambient pressure. Thus, the energy capacity of this nitrogen nanotube is

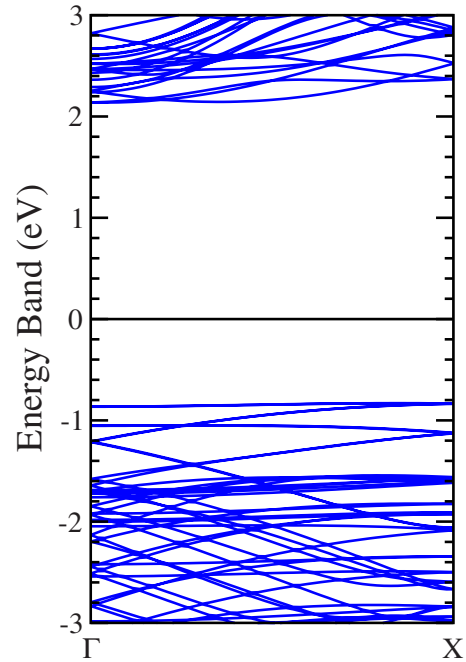


FIG. 5. (Color online) The band structure of the nitrogen nanotube calculated at ambient pressure with an energy band gap of about 3.0 eV .

about 1.378 kJ/g higher than that of nitrogen CG considering potential high energetic materials.

It is challenging to experimentally synthesize this novel polymeric nitrogen nanotube since the layered ZS phase is required. Based on the calculations, synthesis of the ZS phase from denser nitrogen molecular phases will need about 200 GPa pressure along with lower temperature. In general, transformations of zigzag chainlike phases are theoretically found much more favorable in cold compression than other polymeric nitrogen phases. Thus, prevention of any transformation of zigzag chainlike phases in cold compression is one of the key issues in experimental synthesis of this nitrogen nanotube.

IV. CONCLUSION

We have presented an example of a metastable nanotube composed of nitrogen atoms alone. This nitrogen nanotube is wrapped with our recently predicted stable layered polymeric nitrogen phase, which is transformed from denser molecular nitrogen structures in cold compression. The metastability of the nitrogen tube was confirmed by both a phonon-dispersion curve and molecular dynamics calculations at room temperature. Their structural properties have been described together with the band structure. A brief discussion on the possibility of experimental synthesis of the pure nitrogen nanotube was also included.

- ¹C. Mailhiot, L. H. Yang, and A. K. McMahan, *Phys. Rev. B* **46**, 14419 (1992).
- ²M. I. Eremets, A. G. Gavriliuk, I. A. Trojan, D. A. Dzivenko, and R. Boehler, *Nature Mater.* **3**, 558 (2004).
- ³F. Zahariev, S. V. Dudiy, J. Hooper, F. Zhang, and T. K. Woo, *Phys. Rev. Lett.* **97**, 155503 (2006).
- ⁴W. D. Mattson, D. Sanchez-Portal, S. Chiesa, and R. M. Martin, *Phys. Rev. Lett.* **93**, 125501 (2004).
- ⁵R. J. Bartlett, *Chem. Ind.* **4**, 140 (2000).
- ⁶D. L. Strout, *J. Phys. Chem. A* **109**, 1478 (2005).
- ⁷J. S. Wright, D. J. McKay, and G. A. DiLabio, *J. Mol. Struct.: THEOCHEM* **424**, 47 (1998).
- ⁸A. A. Bliznyuk, M. Shen, and H. F. Schaefer III, *Chem. Phys. Lett.* **198**, 249 (1992).
- ⁹M. R. Manaa, *Chem. Phys. Lett.* **331**, 262 (2000).
- ¹⁰L. J. Wang and M. Z. Zgierski, *Chem. Phys. Lett.* **376**, 698 (2003).
- ¹¹F. Zahariev, A. Hu, J. Hooper, F. Zhang, and T. K. Woo, *Phys. Rev. B* **72**, 214108 (2005).
- ¹²J. Kotakoski and K. Albe, *Phys. Rev. B* **77**, 144109 (2008).
- ¹³S. Iijima, *Nature (London)* **354**, 56 (1991).
- ¹⁴D. Golberg, W. Han, Y. Bando, L. Bourgeois, K. Kurashima, and T. Sato, *J. Appl. Phys.* **86**, 2364 (1999).
- ¹⁵H. J. Xiang, J. Yang, J. G. Hou, and Q. Zhu, *Phys. Rev. B* **68**, 035427 (2003).
- ¹⁶I. Cabria, J. A. Alonso, and M. J. López, *Phys. Status Solidi* **203**, 1105 (2006).
- ¹⁷S. Azevedo and R. de Paiva, *Europhys. Lett.* **75**, 126 (2006).
- ¹⁸M. Terrones, A. M. Benito, C. Manteca-Diego, W. K. Hsu, O. I. Osman, J. P. Hare, D. G. Reid, H. Terrones, A. K. Cheetham, K. Prassides, H. W. Kroto, and D. R. M. Walton, *Chem. Phys. Lett.* **257**, 576 (1996).
- ¹⁹L. G. Bulusheva, A. V. Okotrub, A. G. Kudashov, I. P. Asanov, and O. G. Abrosimov, *Eur. Phys. J. D* **34**, 271 (2005).
- ²⁰G. Seifert and E. Hernández, *Chem. Phys. Lett.* **318**, 355 (2000).
- ²¹I. Cabria and J. W. Mintmire, *Europhys. Lett.* **65**, 82 (2004).
- ²²G. Seifert, T. Heine, and P. W. Fowler, *Eur. Phys. J. D* **16**, 341 (2001).
- ²³J. L. Wang, F. H. Lushington, and P. G. Mezey, *J. Chem. Inf. Model.* **46**, 1965 (2006).
- ²⁴J. P. Perdew, K. Burke, and M. Ernzerhof, *Phys. Rev. Lett.* **77**, 3865 (1996).
- ²⁵J. Soler, E. Artacho, J. Gale, A. Garcia, J. Junquera, P. Ordejon, and D. Sanchez-Portal, *J. Phys.: Condens. Matter* **14**, 2745 (2002).
- ²⁶G. Kresse and J. Furthmüller, *Phys. Rev. B* **54**, 11169 (1996).
- ²⁷D. R. Hamann, M. Schlüter, and C. Chiang, *Phys. Rev. Lett.* **43**, 1494 (1979).
- ²⁸N. Troullier and J. Martins, *Phys. Rev. B* **43**, 1993 (1991).
- ²⁹J. Junquera, O. Paz, D. Sanchez-Portal, and E. Artacho, *Phys. Rev. B* **64**, 235111 (2001).
- ³⁰P. E. Blöchl, *Phys. Rev. B* **50**, 17953 (1994).
- ³¹K. Kunc and R. M. Martin, *Phys. Rev. Lett.* **48**, 406 (1982).
- ³²J. Hooper, A. Hu, F. Zhang, and T. K. Woo, *Phys. Rev. B* **80**, 104117 (2009).
- ³³A. F. Goncharov, E. Gregoryanz, H. K. Mao, Z. Liu, and R. J. Hemley, *Phys. Rev. Lett.* **85**, 1262 (2000).